

See discussions, stats, and author profiles for this publication at: <https://www.researchgate.net/publication/24210646>

In Situ Lipidomic Analysis of Nonalcoholic Fatty Liver by Cluster TOF-SIMS Imaging

ARTICLE *in* ANALYTICAL CHEMISTRY · APRIL 2009

Impact Factor: 5.64 · DOI: 10.1021/ac900045m · Source: PubMed

CITATIONS

83

READS

88

5 AUTHORS, INCLUDING:



[Delphine Debois](#)

ZenTech S.A.

26 PUBLICATIONS 546 CITATIONS

[SEE PROFILE](#)



[Alain Brunelle](#)

French National Centre for Scientific Resea...

157 PUBLICATIONS 3,638 CITATIONS

[SEE PROFILE](#)



[Olivier Laprévote](#)

Université René Descartes - Paris 5

245 PUBLICATIONS 4,184 CITATIONS

[SEE PROFILE](#)

Anal. Chem. **2009**, *81*, 2823–2831

Accelerated Articles

In Situ Lipidomic Analysis of Nonalcoholic Fatty Liver by Cluster TOF-SIMS Imaging

Delphine Debois,^{†,‡} Marie-Pierre Bralet,^{§,¶,||} François Le Naour,^{||,¶} Alain Brunelle,^{*,†} and Olivier Laprévote^{†,○}

Institut de Chimie des Substances Naturelles, CNRS, UPR 2301, Avenue de la Terrasse, 91198 Gif-sur-Yvette Cedex, France, AP-HP Hôpital Paul Brousse, Service Anatomie Pathologique, 94807 Villejuif, France, Université Paris-Sud, Institut André Lwoff, F-94807 Villejuif, France, Inserm U785, F-94807 Villejuif, France, Inserm U602, F-94807 Villejuif, France, and Laboratoire de Toxicologie, IFR 71, Faculté des Sciences Pharmaceutiques et Biologiques, Université Paris Descartes, 4, Avenue de l'Observatoire, 75006 Paris, France

Mass spectrometry imaging has been used to map liver biopsies of several patients suffering from nonalcoholic fatty liver disease. This steatosis is characterized by an accumulation of triacylglycerols and diacylglycerols in the liver. Using time-of-flight-secondary ion mass spectrometry (TOF-SIMS) with a bismuth cluster ion source, it has been possible to map lipids *in situ* at the micrometer scale and to simultaneously characterize their molecular distribution on liver sections. Accumulation of triacylglycerols, diacylglycerols, monoacylglycerols, fatty acids, with the apparition of myristic acid, together with a dramatic depletion of vitamin E and a selective macrovacuolar localization of cholesterol are observed in steatosis areas of fatty livers compared to control livers. These ion species are concentrated in small vesicles having a size of a few micrometers. Moreover, very fine differences in lipid localizations, depending on alkyl acid chain lengths of diacylglycerols and fatty acids, have been found after careful scrutiny of the ion images. Finally, TOF-SIMS has revealed lipid zonation in the normal human liver and accumulation of very similar lipids to those detected in areas of the fatty livers, which are not characterized as steatotic ones by the histological control performed on serial tissue sections.

Nonalcoholic fatty liver disease (NAFLD) describes a spectrum of conditions characterized mainly by the histological finding of

hepatic macrovesicular steatosis in patients who consume little or no alcohol.¹ The hallmark of the pathogenesis of NAFLD, both histologically and metabolically, is the accumulation of triacylglycerols (TAG) and diacylglycerols (DAG) in the liver. This storage results from an imbalance in the uptake, synthesis, export, and oxidation of fatty acids.^{2,3} However, the primary metabolic abnormalities leading to lipid accretion are not well understood. To clarify the earliest events in TAG accumulation, analysis of patients with simple fatty livers (i.e., without hepatitis) is needed. The relative contribution of the various pathways in hepatic lipid metabolism to the development of a fatty liver and disturbances in very low density lipoproteins (VLDL) production are poorly understood but may, at least in part, be related to the localization of these processes within the liver. In the liver parenchyma, the key enzymes of various pathways and thus the metabolic capacities are asymmetrically distributed. As an example, the capacity for oxidative energy metabolism, glucose output, and urea synthesis is greater in the periportal area, whereas the capacity for glucose uptake, glutamine formation, and xenobiotic metabolism is higher in the perivenous area.⁴ Specific isolation of hepatocytes from perivenous areas and from periportal areas revealed that fatty acid (FA) synthesis and TAG accumulation occur predominantly in the perivenous areas of the liver, whereas FA oxidation is more associated with the periportal areas.⁵ Recently, Puri et al. per-

[¶] Université Paris-Sud.

^{||} Inserm U785.

[○] Inserm U602.

[○] Université Paris Descartes.

(1) Torres, D. M.; Harrison, S. A. *Gastroenterology* **2008**, *134*, 1682–1698.

(2) Ginsberg, H. N. *Cell. Metab.* **2006**, *4*, 179–181.

(3) Goldberg, I. J.; Ginsberg, H. N. *Gastroenterology* **2006**, *130*, 1343–1346.

(4) Jungermann, K.; Kietzmann, T. *Hepatology* **2000**, *31*, 255–260.

(5) Guzman, M.; Castro, J. *Biochem. J.* **1989**, *264*, 107–113.

* To whom correspondence should be addressed. E-mail: Alain.Brunelle@icsn.cnrs.gif.fr. Phone: 33 169 824 575. Fax: 33 169 077 247.

† Institut de Chimie des Substances Naturelles, CNRS, UPR 2301.

‡ Present address: Laboratory of mass spectrometry (GIGA, CART), University of Liège, B-4000 Liège, Belgium.

§ AP-HP Hôpital Paul Brousse.

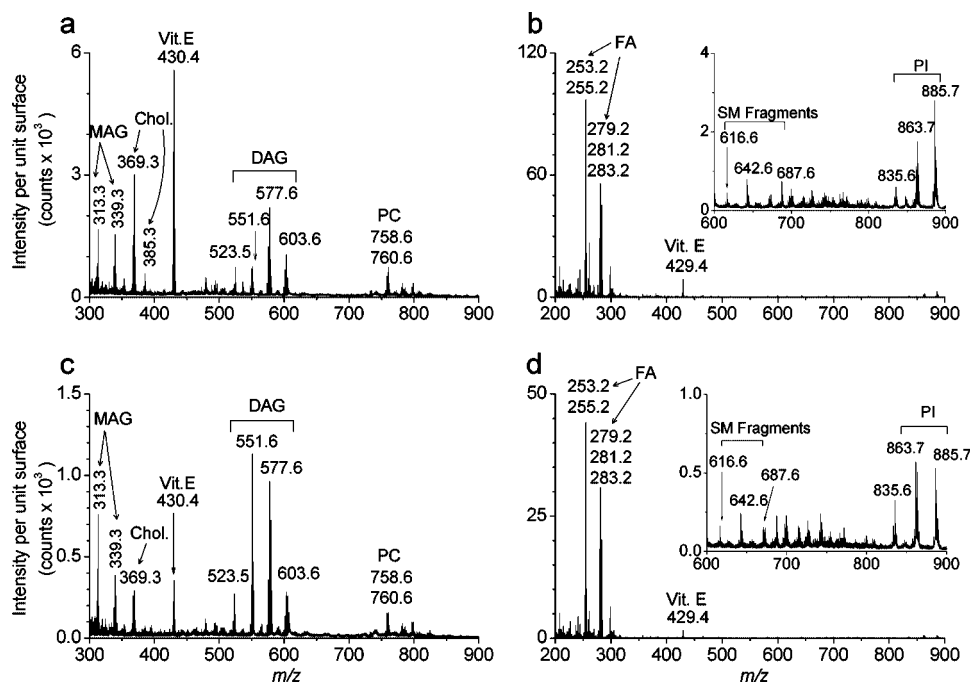


Figure 1. TOF-SIMS mass spectra extracted from two different areas of a healthy liver section: (a) positive ion mode, periportal area, (b) negative ion mode, periportal area, (c) positive ion mode, centrilobular area, (d) negative ion mode, centrilobular area. MAG, monoacylglycerol; Vit.E, vitamin E; Chol., cholesterol; DAG, diacylglycerol; PC, phosphatidylcholine; FA, fatty acid; SM, sphingomyeline; PI, phosphatidylinositol.

formed a lipidomic analysis of nonalcoholic steatohepatitis (NASH) and nonalcoholic fatty liver (NAFL) using capillary gas chromatography on liver extracts.⁶ They observed that NAFLD is associated with numerous changes in the lipid composition of the liver showing a significant stepwise increase in the triacylglycerol/diacylglycerol (TAG/DAG) ratio, in the free cholesterol/phosphatidylcholine ratio from normal liver to NAFL to NASH, and a significant depletion of polyunsaturated fatty acid content of TAG in NAFL and NASH compared to normal liver. Unfortunately, spatial distributions of the specific types of lipids into the tissue could not be obtained with such an approach.

Imaging techniques based on mass spectrometry, i.e., matrix-assisted laser desorption/ionization-time-of-flight mass spectrometry^{7,8} (MALDI-TOF MS) and time-of-flight-secondary ion mass spectrometry⁹ (TOF-SIMS) have been developed or improved for the last 10 years. These techniques allow the mapping of any compound present at the surface of a tissue section.^{10–13} Tissue sections are divided into pixels, and a mass spectrum is recorded for each one. The intensity of a compound of interest, which is depicted by a color scale, is associated with the spatial coordinates of each pixel. For mass spectrometry imaging (MSI), data processing

(image reconstruction) is done with specialized software by integrating signal intensities at desired m/z values across the data set. The systematic investigation of the section allows the construction of ion density maps, or specific molecular images, for virtually every signal detected during the analysis. In TOF-SIMS, the sample is bombarded with primary ions (heavy metal clusters and fullerenes are the most popular)^{13,14} to desorb and ionize the molecules present at the surface of the sample, and the so-called secondary ions are analyzed by their time-of-flight, which is linearly linked to the square root of the m/z ratio. Thanks to the recent improvements in sensitivity,^{15–17} TOF-SIMS imaging is now used in microbiology¹⁸ or in biomedical research.^{13,19–24} The accessible mass range is about 1200 Da, which makes it very suitable for small molecule analysis such as lipids. In addition, the routine spatial resolution of TOF-SIMS imaging is on the order of the micrometer, allowing analysis at the cellular and subcellular levels.^{12,13}

In order to determine the lipid composition of fatty liver, we performed an *in situ* lipidomic analysis using TOF-SIMS imaging. The aim of our study was to assess the composition and local

- (6) Puri, P.; Baillie, R. A.; Wiest, M. M.; Mirshahi, F.; Choudhury, J.; Cheung, O.; Sargeant, C.; Contos, M. J.; Sanyal, A. J. *Hepatology* **2007**, *46*, 1081–1090.
- (7) Karas, M.; Bachmann, D.; Bahr, U.; Hillenkamp, F. *Int. J. Mass Spectrom. Ion Processes* **1987**, *78*, 53–68.
- (8) Karas, M.; Hillenkamp, F. *Anal. Chem.* **1988**, *60*, 2299–2301.
- (9) Chait, B. T.; Standing, K. G. *Int. J. Mass Spectrom. Ion Phys.* **1981**, *40*, 185–193.
- (10) McDonnell, L. A.; Heeren, R. M. A. *Mass Spectrom. Rev.* **2007**, *26*, 606–643.
- (11) Stoeckli, M.; Chaurand, P.; Hallahan, D. E.; Caprioli, R. M. *Nat. Med.* **2001**, *7*, 493–496.
- (12) Brunelle, A.; Touboul, D.; Laprévote, O. *J. Mass Spectrom.* **2005**, *40*, 985–999.
- (13) Brunelle, A.; Laprévote, O. *Curr. Pharm. Design* **2007**, *13*, 3335–3343.
- (14) Weibel, D.; Wong, S.; Lockyer, N.; Blenkinsopp, P.; Hill, R.; Vickerman, J. C. *Anal. Chem.* **2003**, *75*, 1754–1764.
- (15) Touboul, D.; Halgand, F.; Brunelle, A.; Kersting, R.; Tallarak, E.; Hagenhoff, B.; Laprévote, O. *Anal. Chem.* **2004**, *76*, 1550–1559.
- (16) Sjövall, P.; Lausmaa, J.; Johansson, B. *Anal. Chem.* **2004**, *76*, 4271–4278.
- (17) Touboul, D.; Kollmer, F.; Niehuis, E.; Brunelle, A.; Laprévote, O. *J. Am. Soc. Mass Spectrom.* **2005**, *16*, 1608–1618.
- (18) Debois, D.; Hamzé, K.; Guérineau, V.; Le Caë, J. P.; Holland, I. B.; Lopes, P.; Ouazzani, J.; Séror, S. J.; Brunelle, A.; Laprévote, O. *Proteomics* **2008**, *8*, 3682–3691.
- (19) Nygren, H.; Malmberg, P. *Trends Biotechnol.* **2007**, *25*, 499–504.
- (20) Tahallah, N.; Brunelle, A.; De La Porte, S.; Laprévote, O. *J. Lipid Res.* **2008**, *49*, 438–454.
- (21) Magnusson, Y.; Friberg, P.; Sjövall, P.; Dangardt, F.; Malmberg, P.; Chen, Y. *Clin. Physiol. Funct. Imaging* **2008**, *28*, 202–209.
- (22) Malmberg, P.; Nygren, H.; Richter, K.; Chen, Y.; Dangardt, F.; Friberg, P.; Magnusson, Y. *Microsc. Res. Tech.* **2007**, *70*, 828–835.

Table 1. Main Lipid Positive and Negative Ion Species Assigned *In Situ* by TOF-SIMS on the Liver Sections

ion species	experimental <i>m/z</i>	theoretical <i>m/z</i>	assignment
MAGs	311.24	311.26	MAG (16:1) [M + H - H ₂ O] ⁺
	313.28	313.27	MAG (16:0)
	339.29	339.29	MAG (18:1)
	341.32	341.31	MAG (18:0)
DAGs	519.45	519.44	DAG (30:2) [M + H - H ₂ O] ⁺
	521.48	521.46	DAG (30:1)
	523.51	523.47	DAG (30:0)
	547.50	547.47	DAG (32:2)
	549.54	549.49	DAG (32:1)
	551.57	551.50	DAG (32:0)
	573.52	573.49	DAG (34:3)
	575.54	575.5	DAG (34:2)
	577.56	577.52	DAG (34:1)
	599.51	599.50	DAG (36:4)
TAGs	601.54	601.52	DAG (36:3)
	603.55	603.54	DAG (36:2)
	851.70	851.71	TAG (50:3) [M + Na] ⁺
	853.75	853.73	TAG (50:2)
	855.79	855.74	TAG (50:1)
	857.80	857.76	TAG (50:0)
	877.72	877.73	TAG (52:4)
	879.76	879.74	TAG (52:3)
	881.78	881.76	TAG (52:2)
	883.81	883.77	TAG (52:1)
cholesterol	885.81	885.79	TAG (52:0)
	369.36	369.35	cholesterol [M + H - H ₂ O] ⁺
vitamin E	385.34	385.35	cholesterol [M-H] ⁻
	430.37	430.38	vitamin E M ⁺ *
PC	758.59	758.57	GPCho (16:0/18:2) [M + H] ⁺
	760.55	760.59	GPCho (16:0/18:1)
FAs	227.2	227.2	FA 14:0 [M - H] ⁻
	253.22	253.22	FA 16:1
	255.23	255.23	FA 16:0
	279.22	279.23	FA 18:2
	281.23	281.25	FA 18:1
	283.24	283.26	FA 18:0
vitamin E SM 34:1	429.37	429.37	vitamin E [M - H] ⁻
	616.49	616.47	[M - (C ₂ H ₂ (N(CH ₃) ₃))] ⁻
	642.55	642.49	SM d18:1/16:0 [M - (N(CH ₃) ₃)] ⁻
	687.63	687.55	[M - CH ₃] ⁻
PIs	885.68	885.55	GPIns (18:0/20:4) M ⁻
	887.67	887.56	GPIns (18:0/20:3)

distribution of lipids directly on liver tissue sections from patients with steatosis.

MATERIALS AND METHODS

Origin of Samples and Patient History. Liver specimens were obtained from the Centre de Ressources Biologiques Paris-Sud (Paris-Sud XI University, France). Access to this material was in agreement with French ethical laws. Tissues were sampled from liver resection on seven patients (mean age, 52 years; range, 36–71 years) who underwent surgery for focal nodular hyperplasia (*n* = 2), liver hemangioma (*n* = 1), gallbladder carcinoma (*n* = 3), and hepatic colon metastasis (*n* = 1). For all patients, daily alcohol consumption was lower than 20 g. Tissues from patients suffering from an infection with hepatitis B virus (HBV) or hepatitis C virus (HCV), genetic hemochromatosis, autoimmune liver diseases, and Wilson's disease were excluded. Tissues were fixed in formalin for routine pathological assessment and one

(23) Mas, S.; Touboul, D.; Brunelle, A.; Aragoncillo, P.; Egido, J.; Laprévote, O.; Vivanco, F. *Analyst* 2007, 132, 24–26.

(24) Malmberg, P.; Börner, K.; Chen, Y.; Friberg, P.; Hagenhoff, B.; Måansson, J. E.; Nygren, H. *Biochim. Biophys. Acta* 2007, 1771, 185–195.

specimen of nontumorous liver distant to the tumor was immediately snap frozen in liquid nitrogen and stored at –80 °C until use. The livers from two of the patients were histologically normal. For five patients, microscopic analysis revealed bland macrovesicular steatosis ranging between 10 and 40%, without hepatocyte ballooning, lobular inflammation, perisinusoidal fibrosis, or Mallory's hyaline.

Tissue Preparation. Serial sections (10 μm thick) were cut at –20 °C with a CM3050-S cryostat (Leica Microsystèmes SAS, France) and alternately deposited on glass slides for extemporaneous histological control and on silicon wafers for TOF-SIMS imaging (2 in. diameter polished silicon wafers, ACM, Villiers Saint Frédéric, France). The main benefits of using silicon wafers are the following: the surface is absolutely flat, is free of contaminants for SIMS (no alkali ions in positive ion mode, no metal oxide ions in negative ion mode), and is conductive. Finally, silicon wafers are relatively cheap and disposable after a single use, avoiding potential contaminations from one experiment to another. Sections for histology were stained with Hematoxylin Eosin Saffron and those for TOF-SIMS imaging were dried under a pressure of a few hectopascals for 30 min, without any further treatment. Before introduction of the sample in the mass spectrometer, reference images of both sections were taken with an Olympus BX51 microscope (Rungis, France), equipped with 1.25× to 50× lenses and a Color View I camera, monitored by Cell^B software (Soft Imaging System GmbH, Münster, Germany). Inside the TOF-SIMS mass spectrometer, video images taken with a small field of view of 1 × 1 mm² were recorded with an integrated camera.

Instrumentation. A standard commercial ToF-SIMS IV (Ion-Tof GmbH, Münster, Germany) reflectron-type TOF mass spectrometer was used for MSI experiments. The primary ion source was a bismuth liquid metal ion gun. Bi₃⁺ cluster ions were selected. The ion column focusing mode ensured both a 1–2 μm beam focus and short pulse duration of less than 1 ns. Such short pulses are a prerequisite for high mass resolution, accurate mass measurements, and structure assignments. Because of the very low initial kinetic energy distribution of the secondary ions, the relationship between the time-of-flight and the square root of *m/z* is always linear over the whole mass range. The mass calibration was always internal and signals used for initial calibration were those of H⁺, H₂⁺, H₃⁺, C⁺, CH⁺, CH₂⁺, and CH₃⁺ for the positive ion mode and the signals of C⁻, CH⁻, C₂⁻, and C₂H⁻ for the negative ion mode. Signals of cholesterol, vitamin E, and diacylglycerols were used for the positive ion mode calibration refinement, and for negative ion mode, fatty acid carboxylate ions, and vitamin E deprotonated molecule were selected. Structure attributions or assignments of ion peaks were made according to the instrument resolution (*M/ΔM* = 10⁴, full width half-maximum [fwhm], at *m/z* 500), accuracy, and the valence rule. Moreover, mass spectra of reference compounds have been recorded and compared to spectra recorded “*in situ*” to confirm the assignments. Finally, the biological relevance of the attribution was also taken into account and many mass assignments were also confirmed or at least reinforced with the help of the literature.^{15,16,19,20,25–28}

(25) Touboul, D.; Brunelle, A.; Halgand, F.; De La Porte, S.; Laprévote, O. *J. Lipid Res.* 2005, 46, 1388–1395.

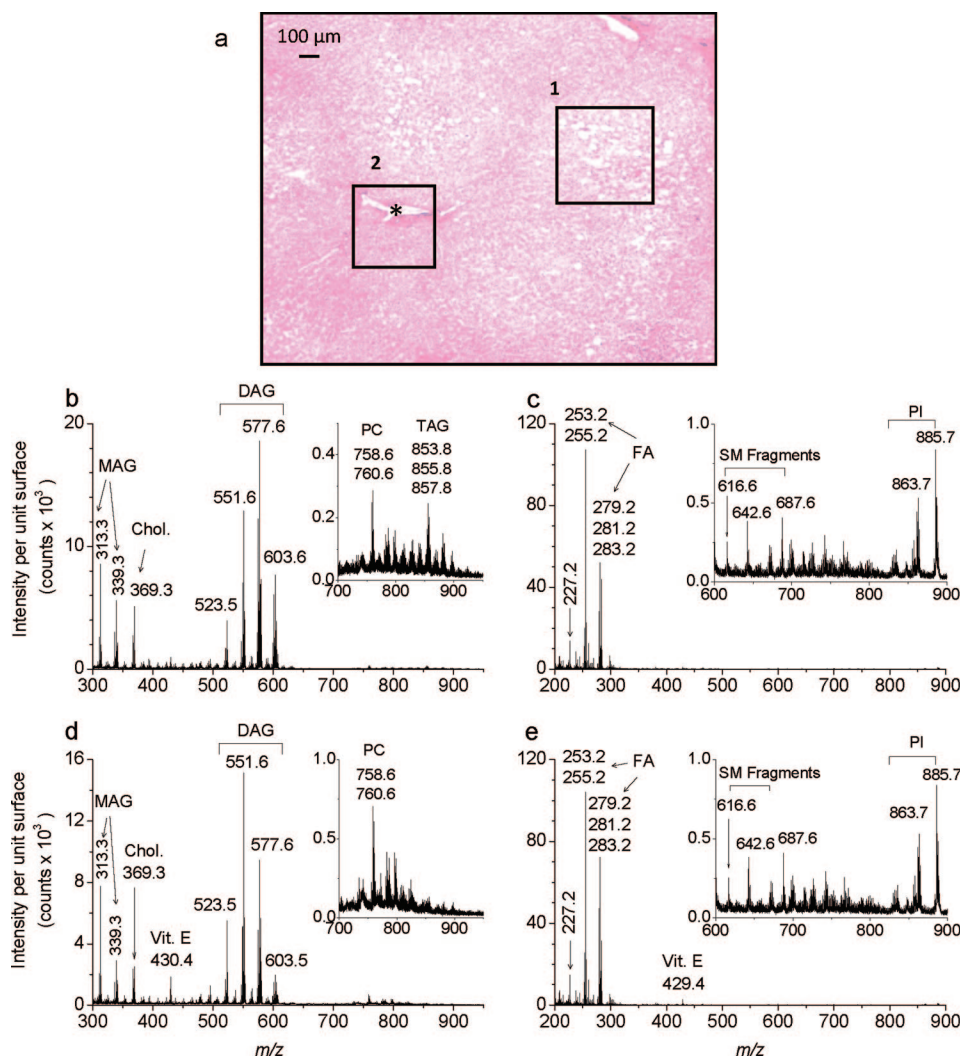


Figure 2. Microscopic picture and TOF-SIMS mass spectra of a fatty liver section. (a) H and E stained fatty liver section. Square 1 is a steatosis area, and square 2 is a nonsteatosis area. * indicates the portal tract. (b–e) TOF-SIMS mass spectra extracted from two different areas inside the steatosis and nonsteatosis areas: (b) positive ion mode, steatosis area, (c) negative ion mode, steatosis area, (d) positive ion mode, nonsteatosis area, (e) negative ion mode, nonsteatosis area. MAG, monoacylglycerol; Vit.E, vitamin E; Chol, cholesterol; DAG, diacylglycerol; TAG, triacylglycerol; PC, phosphatidylcholine; FA, fatty acid; SM, sphingomyeline; PI, phosphatidylinositol.

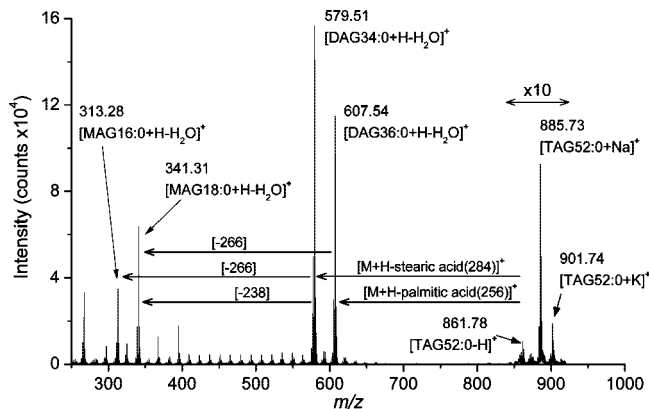


Figure 3. TOF-SIMS positive ion mass spectrum of triacylglycerol TAG52:0 (MW 862.80 Da) solution deposited on a silicon wafer. The neutral losses of 238 and 266 Da correspond to the loss of the ketenes from palmitic and stearic acids.

Images were recorded with a field of view of $500 \times 500 \mu\text{m}^2$ and 256×256 pixels, giving a pixel size of $2 \times 2 \mu\text{m}^2$. A color scale bar, for which the amplitude, in counts, is given for each image, is placed to the right of the ion images. The data

acquisition and processing softwares were IonSpec and IonImage (Ion-Tof GmbH, Münster, Germany).

Positive ion mode and negative ion mode images were successively recorded for each selected area. All the images were recorded with a primary ion fluence (also called primary ion dose density) of 3×10^{11} ions cm^{-2} , well below the so-called static-SIMS limit, ensuring little sample damage and the maximum of intact secondary ion emission for the recording of two successive images on the same area.²⁹ A low-energy electron flood gun was activated to neutralize the surface during the analysis.³⁰

We concentrated our study on the normal and steatotic human liver. In order to focus on specific areas of the tissue such as the periportal and centrilobular areas in the normal liver as well as the steatotic areas in the fatty liver, it was necessary to manually

- (26) Touboul, D.; Piednoël, H.; Voisin, V.; De La Porte, S.; Brunelle, A.; Halgand, F.; Laprévote, O. *Eur. J. Mass Spectrom.* **2004**, *10*, 657–664.
- (27) Monroe, E. B.; Jurchen, J. C.; Lee, J.; Rubakhin, S. S.; Sweedler, J. V. *J. Am. Chem. Soc.* **2005**, *127*, 12152–12153.
- (28) Börner, K.; Nygren, H.; Hagenhoff, B.; Malmberg, P.; Tallarek, E.; Måansson, J. E. *Biochim. Biophys. Acta* **2006**, *1761*, 335–344.

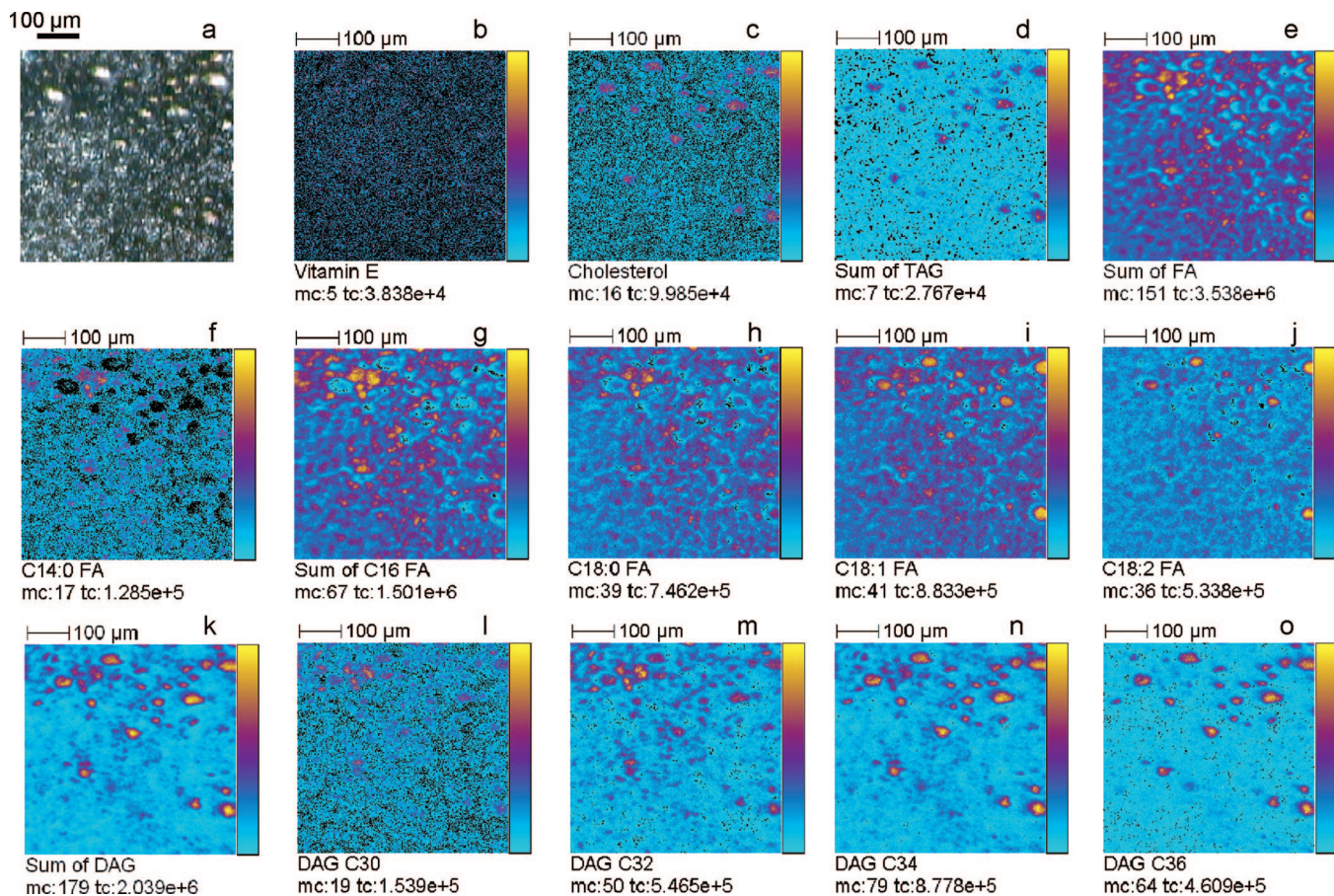


Figure 4. TOF-SIMS imaging of a steatosis area: (a) video image of the steatotic area. Ion images of 14 different positive and negative secondary ions from this area. (b) Vitamin E (negative ion mode), (c) cholesterol (positive ion mode), (d) sum of triacylglycerol ions (TAG, positive ion mode), (e) sum of all fatty acid carboxylate ions (FA, negative ion mode), (f) C14:0 FA (negative ion mode), (g) sum of C16 fatty acid carboxylate ions (negative ion mode), (h) C18:0 FA (negative ion mode), (i) C18:1 FA (negative ion mode), (j) C18:2 FA (negative ion mode), (k) sum of diacylglycerol ions (DAG, positive ion mode), (l) sum of DAG with 30 carbon atoms (DAG C30, positive ion mode), (m) sum of DAG with 32 carbon atoms (DAG C32, positive ion mode), (n) sum of DAG with 34 carbon atoms (DAG C34, positive ion mode); (o) sum of DAG with 36 carbon atoms (DAG C36, positive ion mode). Color scale bars, with amplitude in number of counts, are indicated to the right of each ion image. The amplitude of the color scale corresponds to the maximum number of counts mc and could be read as [0, mc]. tc is the total number of counts recorded for the specified m/z (it is the sum of counts in all the pixels). Field of view: $500 \times 500 \mu\text{m}^2$.

select (with the imaging software) regions of interest (ROIs) corresponding to these areas. The associated mass spectra were further extracted in order to obtain the subsequent local information, leading to more precise localizations and relative intensities. For a proper and easier comparison, as each ROI had a different area (in pixels), a normalization of their respective mass spectrum intensities had to be performed. The intensity of the mass spectrum from each ROI was normalized as if it was composed of the same number of pixels as the smallest one, i.e., the one of the nonsteatosis region.

Pure reference lipid compounds of palmitic acid (C16:0, MW 256.24 Da), stearic acid (C18:0, MW 284.24 Da), arachidonic acid (C20:4, MW 304.24 Da), and triacylglycerol TAG (18:0/18:0/16:0) (TG52:0, MW 862.80 Da) were purchased from Sigma-Aldrich (BP 701 F-38297 St. Quentin Fallavier, France). Solutions were prepared in $\text{CHCl}_3/\text{CH}_3\text{OH}$ 50/50 (v/v) solution. The three FA equimolar mixture contained 17 mmol L^{-1} of each, and the solution of TAG52:0 had a concentration of 1 mmol L^{-1} . A

volume of 1 μL of each solution was deposited on the surface of a silicon wafer, and mass spectra were recorded with a primary ion fluence of $2.5 \times 10^{10} \text{ ions cm}^{-2}$, over an area of $500 \times 500 \mu\text{m}^2$.

RESULTS AND DISCUSSION

To address lipid zonation in the human liver, *in situ* lipidomic investigations were performed on tissue sections using TOF-SIMS. Indeed, differential protein expression³¹ and metabolic activity have already been demonstrated to exist between the periportal and centrilobular (perivenous) hepatocytes. Mass spectra and images were acquired from four sections of two different normal livers including four periportal areas and three centrilobular areas. Figure 1 shows the mass spectra extracted from ROIs corresponding to the periportal and centrilobular areas in both positive and negative ion modes, respectively. The names and m/z values of the ions corresponding to assigned compounds are listed in Table 1. We detected in both regions the same lipid classes with variations of their relative intensities. In the positive ion mode,

(29) Vickerman, J. C. TOF-SIMS: An Overview. In *ToF-SIMS-Surface Analysis by Mass Spectrometry*; Vickerman, J. C., Briggs, D., Eds.; Surface Spectra and IM Publications: Manchester and Chichester, U.K., 2001; pp 1–40.
 (30) Gilmore, I. S.; Seah, M. P. *Appl. Surf. Sci.* **2002**, 187, 89–100.

(31) Braeuning, A.; Ittrich, C.; Köhle, C.; Hailfinger, S.; Bonin, M.; Buchmann, A.; Schwarz, M. *FEBS J.* **2006**, 273, 5051–5061.

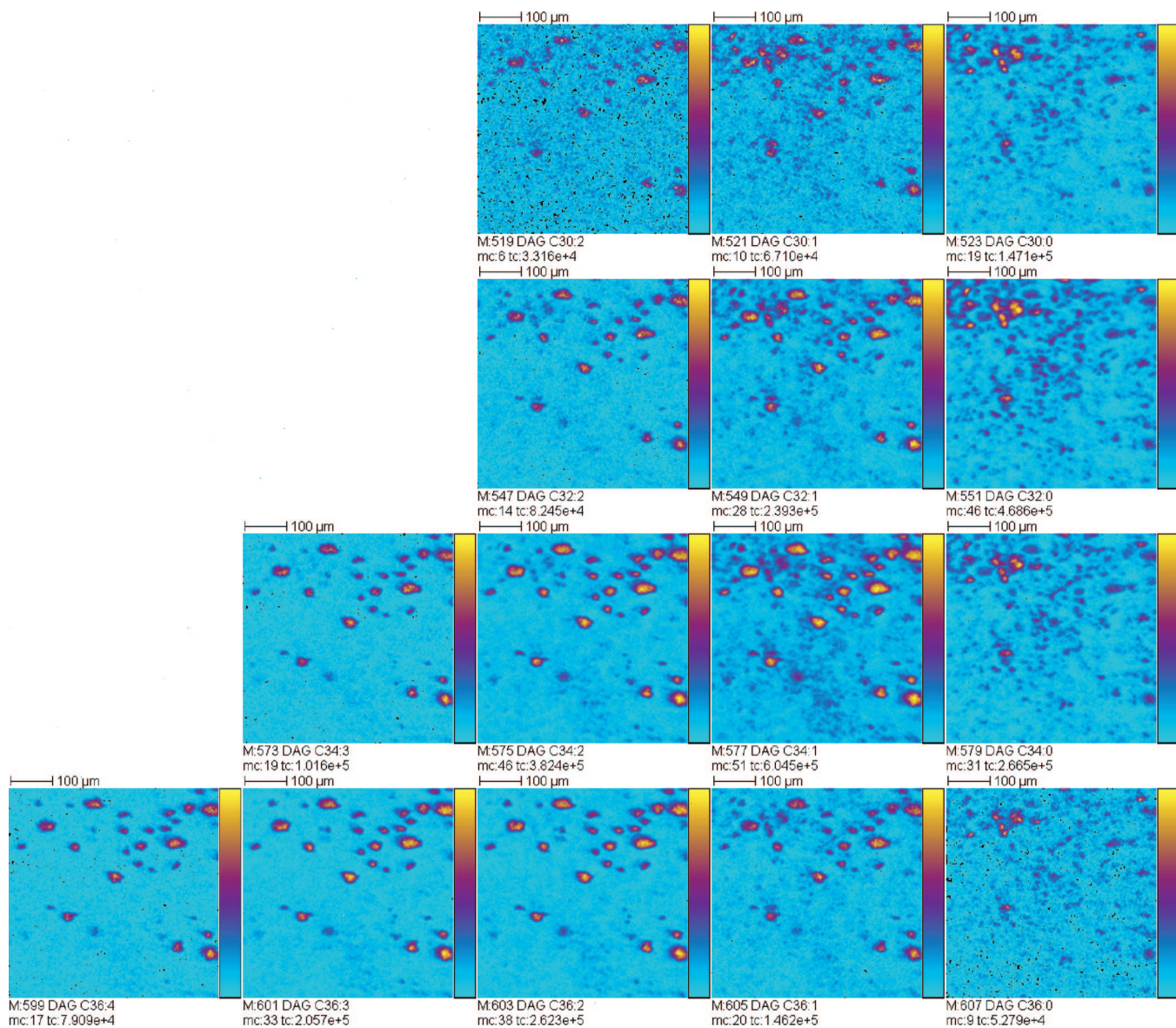


Figure 5. Diacylglycerol positive ion images recorded from a steatosis area of a steatotic liver positive ion analysis. Color scale bars, with amplitude in number of counts, are indicated to the right of each ion image. The amplitude of the color scale corresponds to the maximum number of counts mc and could be read as [0, mc]. tc is the total number of counts recorded for the specified m/z (it is the sum of counts in all the pixels). Field of view $500 \times 500 \mu\text{m}^2$.

we observed monoacylglycerols (m/z 313.28 and 339.29) and cholesterol (m/z 369.36 and m/z 385.33). Vitamin E (more precisely α -tocopherol) is detected at m/z 430.37. Diacylglycerols (DAG) bearing 30, 32, 34, and 36 carbon atoms are also detected at m/z 523.51, 551.57, 577.56, and 603.55, respectively. The last species observed in the positive ion mass spectrum are the phosphatidylcholines (PC) PC 34:2 and PC34:1, detected at m/z 758.59 and 760.55. In the negative ion mode, the most abundant ion peaks are those of fatty acids, bearing 16 and 18 carbon atoms. Signals at m/z 253.22 and 255.23 correspond to carboxylate ions of palmitoleic (C16:1) and palmitic (C16:0) acids, respectively, whereas signals at m/z 279.22, 281.23, and 283.24 correspond to carboxylate ions of linoleic (C18:2), oleic (C18:1), and stearic (C18:0) acids, respectively. Surprisingly, no signal from arachidonic acid (C20:4) is observed in the negative ion mode mass spectra, while this species is expected to be present in liver in

amounts comparable to those of C16 and C18 fatty acids. A reference mass spectrum was therefore recorded in the negative ion mode (Figure S-1 in the Supporting Information) from a droplet deposited on a silicon wafer and containing equal amounts of palmitic (C16:0), stearic (C18:0), and arachidonic (C20:4) acids. The signals of the carboxylate ions from these three fatty acids (FAs) present comparable intensities. These observations suggest that most of the observed FA carboxylate ions mainly originate from in-source fragmentation of heavier species such as DAGs or TAGs. However, the C20:4 free fatty acid is not detected by the present method, suggesting that it is not concentrated enough. These results can therefore not be considered as quantitative ones but only as imaging mass spectrometry of lipid species. The $[\text{M} - \text{H}]^-$ ion of the deprotonated vitamin E is detected at m/z 429.37. Only sphingomyelin (d18:1/16:0) (SM (d18:1/16:0)) fragments are detected at m/z 642.55 and 687.63. The last

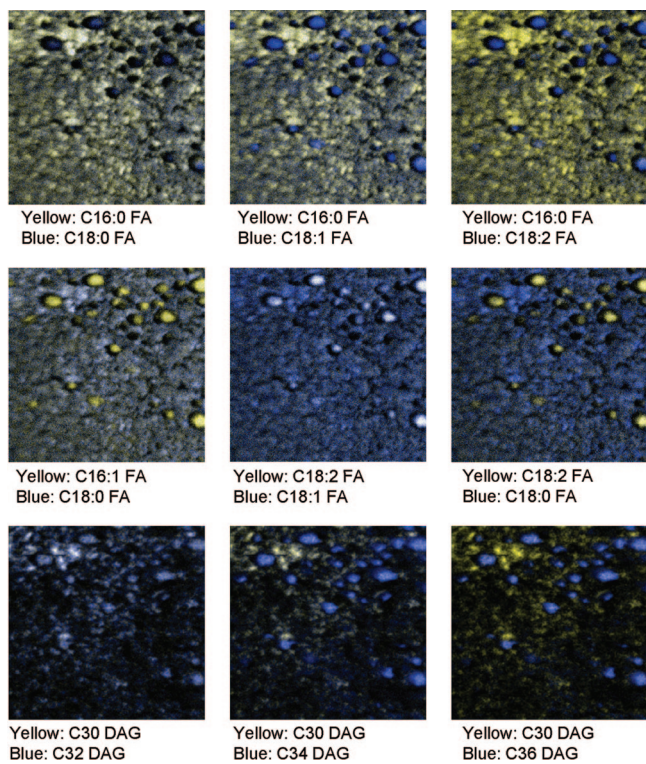


Figure 6. Two color overlays showing the individual localization of different secondary ions.

species observed in the negative ion mass spectrum are phosphatidylinositols (PI) bearing 36 and 38 carbon atoms (m/z 863.68 and 885.67). All these lipid species are present in the two normal human livers studied. A comparison between the periportal and centrilobular zones was further investigated. Thus, in the negative ionization mode, fatty acids are the most predominant ions in the mass spectra whatever the zone, periportal or centrilobular zones. In positive ionization mode, the most abundant ions in the mass spectra are α -tocopherol and cholesterol in periportal zones, whereas DAGs are the most abundant species in centrilobular zones. Altogether, these results suggest that a zonation exists in terms of lipid composition between periportal and centrilobular zones in the liver.

Seven steatosis regions were selected on five steatotic livers exhibiting macrovacuolar steatosis (Figure 2a). Mass spectra and images were acquired using TOF-SIMS mass spectrometry in positive as well as in negative ionization modes (Figure 2b–e). Steatosis is characterized by formation of vesicles that are highly enriched in lipids, in particular DAG and TAG. As expected, these lipids were observed as they are highly abundant. Monoacylglycerols (MAG) and diacylglycerols (DAG) are enriched with the result that DAGs exhibit the most intense signals of the mass spectra. Several molecular species of triacylglycerols (TAG) bearing 50 carbon atoms are also detected. However, DAG species are detected with much higher intensities than TAG despite the major contribution of TAG in the composition of steatotic vesicles.⁶ This apparent discrepancy can be explained by TAG in-source fragmentation yielding MAG and DAG. To confirm this hypothesis, a reference positive ion mode mass spectrum was recorded from pure TG52:0 (Figure 3). It is clear from this mass spectrum that TAG species undergo in-source fragmentation, leading to intense signals of DAG type fragments after the loss of one FA

chain. The DAG species detected in the mass spectra and images from the liver may therefore mainly originate both from existing DAGs or from fragmentation of TAGs,²² although they can also originate from other lipid species such as phosphatidylethanolamines or phosphatidylglycerols.³² Other major changes are also observed in steatosis such as a dramatic decrease of signals coming from vitamin E and the appearance of a signal from the carboxylate ion of myristic acid (C14:0) at m/z 227.20. The distribution of some detected lipids could be precisely distinguished by imaging (Figure 4). Cholesterol, which is more intense in steatotic than in nonsteatotic areas, exhibits selective macrovacuolar distribution (Figure 4c). The sum of TAG species shows a major macrovacuolar distribution and colocalization with cholesterol in steatotic vesicles (Figure 4d). On the other hand, the ion image of the sum of FA (Figure 4e) shows that these compounds are present more homogeneously over the whole analyzed area. Moreover, localizations of each individual FA were investigated in depth revealing important differences in their distribution. Indeed, myristic acid (C14:0), palmitic (C16:0), and palmitoleic acids (C16:1) as well as stearic acid (C18:0) are detected mainly outside of steatotic vesicles (Figures 4f–h) whereas linoleic acid (C18:2) exhibits a specific localization in lipid droplets (Figure 4j). It should be noted that oleic acid (C18:1) displays an intermediate localization (Figure 4i). Furthermore, important differences in the distribution of individual DAG species are also observed. Thus, DAG C30 is detected mainly outside of steatotic vesicles (Figure 4l) whereas DAG C36 is specifically localized in these vesicles (Figure 4o). The DAG C32 and C34 exhibit intermediate distributions in agreement with both their respective FA composition and the FA localizations (parts m and n of Figure 4). In addition, distributions of individual DAG species (C30:2, C30:1, C30:0, C32:2, C32:1, C32:0, C34:3, C34:2, C34:1, C34:0, C36:4; C36:3, C36:2, C36:1, and C36:0), in both areas, could also be precisely drawn (Figure 5) and exhibited different localizations in agreement with both their respective FA composition and the FA localizations of Figure 4. These precise distributions of DAG species reinforce the hypothesis that most of the observed FA carboxylate ions originate from in-source fragmentations of DAGs and TAGs.

In order to confirm the various distributions of different compounds, overlays of respective ion images were also made for some FA and DAG species (Figure 6). This process allows the colocalization of two molecular species to be determined since they appear in two different colors (yellow and blue) when they are not colocalized and any modification of these colors expresses a colocalization. The overlay image obtained from DAG C30 and C32 leads to visualization of lipid droplets in white showing a partial colocalization of these two DAG species. By contrast, the signals of DAG C30 and C36 species are, respectively, yellow and blue, showing that these species present different localizations, without spatial mixing. The C30 and C34 DAG species are observed partially colocalized.

As lipid profiles were obviously different between normal liver and steatosis, we used TOF-SIMS imaging to compare the lipid content and distribution between normal liver and the nonsteatotic part of the fatty liver. In the latter part, we observe an increase of

(32) Luxembourg, S. L.; McDonnell, L. A.; Duursma, M. C.; Guo, X.; Heeren, R. M. A. *Anal. Chem.* 2003, 75, 2333–2341.

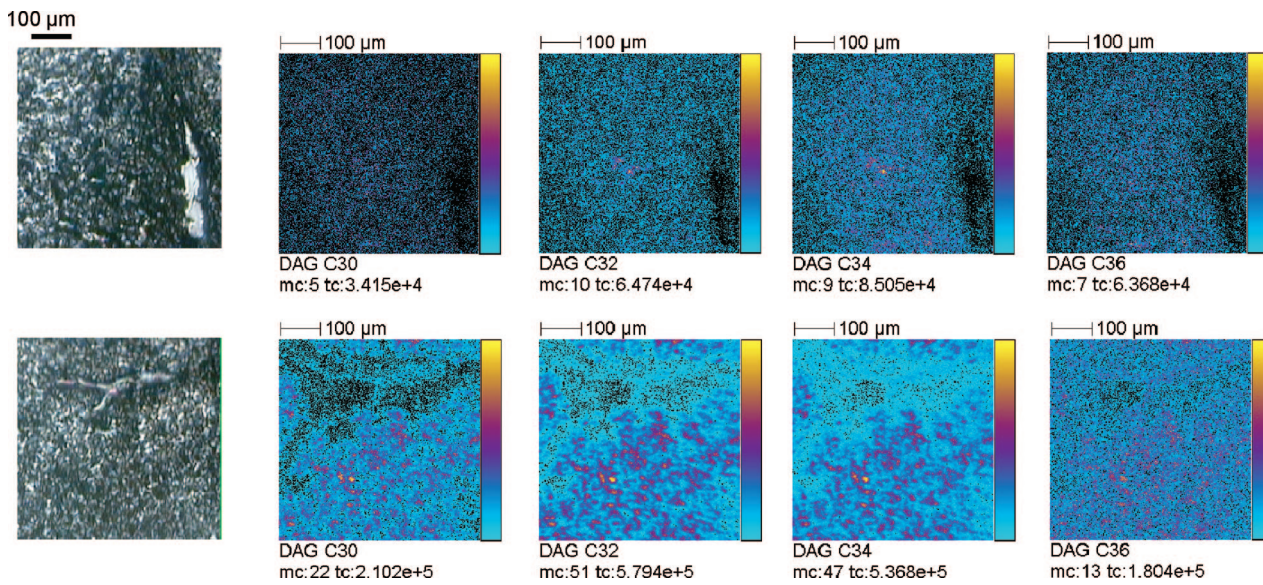


Figure 7. Diacylglycerol ion images in the periportal area of a healthy liver and in the nonsteatosis area of a steatotic liver. Top line: periportal area of a healthy liver, video image and secondary ion images of the sum of diacylglycerol ions with 30, 32, 34, and 36 carbon atoms, respectively (DAG C30, C32, C34, C36). Bottom line: nonsteatosis area of a steatotic liver, video image and same ions. The amplitude of the color scale corresponds to the maximum number of counts mc and could be read as [0, mc]. to is the total number of counts recorded for the specified m/z (it is the sum of counts in all the pixels). Field of view: $500 \times 500 \mu\text{m}^2$.

MAG and DAG (Figures 2 and 7), especially DAG with 30, 32, and 34 carbon atoms, an increase of fatty acids such as oleic acid (C18:1), and the appearance of myristic acid (C14:0). α -Tocopherol as well as SM (d18:1/16:0) and the phosphatidylinositol signals intensities strongly decrease compared to those from normal livers. Distributions of individual DAG species could also be drawn and are shown in Figure S-2 in the Supporting Information. Nevertheless, such variations are lower than those noted in macrovacuolar steatosis.

This is the first *in situ* lipidomic analysis of human liver using TOF-SIMS imaging directly on tissue sections. The strengths of this nondestructive, sensitive, and powerful approach are multiple.^{13,19} It allows the acquisition of lipid profiles of a tissue, while maintaining its topographic integrity, at a micrometer scale resolution. Furthermore, retrospective analyses can be performed after the original raw data has been collected. Nevertheless, some limitations have to be specified. The lack of MS/MS mode or access to ultrahigh mass resolution is problematic when isobaric ions cannot be discriminated. In this case, an *in situ* PSD-like method has been demonstrated to be very useful for lipid identification, as specific fragments are observed, allowing a clear attribution.³³ Finally, TOF-SIMS appears to induce more fragment ions in comparison with other mass spectrometry techniques¹⁰ as exemplified in our study by the very high concentration of DAG detected in macrovesicular steatosis, which could be in part considered as fragments of larger macromolecules such as TAG as they show the same tissue distribution.

Our study demonstrates that healthy normal human liver exhibits lipid zonation since we observed a higher abundance of α -tocopherol and cholesterol in the periportal zones, whereas DAG were the most abundant species in the centrilobular zones. For patients with nonalcoholic steatosis, TOF-SIMS revealed important

changes in lipid composition. Thus, macrovesicles of steatosis are *in situ* mainly composed of cholesterol, TAG, DAG (particularly those with 32, 34, and 36 carbon atoms) and fatty acids, especially oleic acid (C18:1) and linoleic acid (C18:2). TOF-SIMS also revealed important changes in the lipid composition of the nonsteatotic part of fatty liver, reflecting the earliest metabolic disturbances of fatty liver despite similar morphological aspect as compared to healthy liver (histological observation).

Steatosis also exhibits a dramatic decrease in vitamin E, in particular, α -tocopherol. Vitamin E is a group of compounds joining tocopherols and tocotrienols, where α -tocopherol has the highest concentration in the liver.³⁴ TOF-SIMS imaging allowed distribution to be localized, showing a periportal predominance in normal liver and a dramatic decrease in nonalcoholic fatty liver, especially in steatotic vesicles. This potent antioxidant plays a role in protecting cells from injury caused by reactive species of oxygen and lipid peroxidation.³⁵ Its depletion in the liver can be due to its consumption for fighting an oxidative stress. Furthermore, its association with the accumulation of unsaturated long chain fatty acids as shown in steatotic vesicles creates a favorable environment for lipid peroxidation and deleterious consequences on cell and mitochondria membranes.

There are a few studies investigating lipid contents in NAFLD patients that show numerous changes in lipid and hepatic FA composition.^{6,36,37} No absolute quantitative data, such as those given on liver homogenates from patients with NAFLD using capillary gas chromatography^{6,36,37} is obtained by TOF-SIMS, but relative quantification seems to be possible as seen in the images and also in the mass spectra extracted from ROIs. Nevertheless, this relative quantification with TOF-SIMS should be mentioned with great care since in some very specific cases ion suppression effects (called matrix-effects) have been reported.³⁸ As compared to results obtained from liver extracts, some lipids were not

(33) Touboul, D.; Brunelle, A.; Laprévote, O. *Rapid Commun. Mass Spectrom.* 2006, 20, 703–709.

(34) Zingg, J. M. *Mol. Aspects Med.* 2007, 28, 481–506.

(35) Levine, J. E. *J. Pediatr.* 2000, 136, 734–738.

detected *in situ* such as fatty acids with 20 carbon atoms, phosphatidylserine, phosphatidylethanolamine, and others forms of tocopherol (β , γ , δ). This may be due to poor desorption/ionization yields or also to intense fragmentation of these compounds, due to their chemical structure. Nevertheless, the method remains highly informative because the detected compounds, although not fully representative of the entire lipid content, have a high biological significance. Indeed, although the fatty acid compositions from specific lipid classes cannot be determined precisely by our approach, we could assume that part of the FA arise from DAG/TAG as they are strictly colocalized. This emphasizes the complementarity of TOF-SIMS imaging to conventional methods, although a direct comparison with quantitative methods, based on preliminary extraction of the whole tissue content, may be somewhat difficult. Moreover, TOF-SIMS is to date the unique approach for describing without *a priori* knowledge and simultaneously the local distribution of these fatty acid chains as well as other lipids, opening new insights in the understanding of hepatic lipid metabolism in normal and pathological liver.

CONCLUSION

Cluster-TOF-SIMS imaging has enabled us to map lipids *in situ* and to characterize their molecular distribution in liver

-
- (36) Araya, J.; Rodrigo, R.; Videla, L. A.; Thielemann, L.; Orellana, M.; Pettinelli, P.; Ponichik, J. *Clin. Sci.* **2004**, *106*, 635–643.
 - (37) Allard, J. P.; Aghdassi, E.; Mohammed, S.; Raman, M.; Avand, G.; Arendt, B. M.; Jalali, P.; Kandasamy, T.; Prayitno, N.; Sherman, M.; Guindi, M.; Ma, D. W. L.; Heathcote, J. E. *J. Hepatol.* **2008**, *48*, 300–307.
 - (38) Jones, E. A.; Lockyer, N. P.; Kordis, J.; Vickerman, J. C. *J. Am. Soc. Mass Spectrom.* **2007**, *18*, 1559–1567.

sections from patients with nonalcoholic steatosis. It has allowed us to directly and relatively rapidly probe intact biological tissue sections, with a good preservation of the sample molecular and structural integrity. It has been possible to simultaneously analyze different morphological regions at a micrometer scale together with a high molecular specificity and sensitivity, without any prior preparation procedure. This method thus gives a wide amount of information on the local molecular composition within steatotic and nonsteatotic livers and can be recognized as a powerful approach for localized lipidomics studies in liver. It emerges as a promising and highly valuable indicator of the earliest metabolic disturbances of NAFLD.

ACKNOWLEDGMENT

This paper is dedicated to the memory of our late lamented colleague, Marie-Pierre Bralet, who recently passed away. D.D. is indebted to the French Ministère de l'Éducation Nationale for a Ph.D. research fellowship. This work was supported by the European Union (Contract LSHG-CT-2005-518194 COMPUTIS). Many thanks to Alexandre Seyer for preparing some standard samples and to Rowan Dobson and David Touboul for their careful reading of the manuscript.

SUPPORTING INFORMATION AVAILABLE

Additional information as noted in text. This material is available free of charge via the Internet at <http://pubs.acs.org>.

Received for review January 8, 2009. Accepted March 10, 2009.

AC900045M

Supporting information of:

***In situ* lipidomic analysis of non-alcoholic fatty liver by cluster TOF-SIMS imaging**

By

Delphine Debois^{1‡}, Marie-Pierre Bralet^{2,3,4}, François Le Naour^{3,5}, Alain Brunelle^{1} and Olivier Laprévote^{1,6}*

¹Institut de Chimie des Substances Naturelles, CNRS, UPR 2301, Av. de la Terrasse, 91198 Gif-sur-Yvette Cedex, France

²AP-HP Hôpital Paul Brousse, Service Anatomie Pathologique, 94807 Villejuif, France

³Univ. Paris-Sud, Institut André Lwoff, F-94807 Villejuif, France

⁴Inserm U785, F-94807 Villejuif, France

⁵Inserm U602, F-94807 Villejuif, France

⁶Laboratoire de Toxicologie, IFR 71, Faculté des Sciences Pharmaceutiques et Biologiques, Université Paris Descartes, 4, avenue de l'Observatoire, 75006 Paris, France

‡ Present address: Laboratory of mass spectrometry (GIGA, CART), University of Liège, B-4000 Liège, Belgium

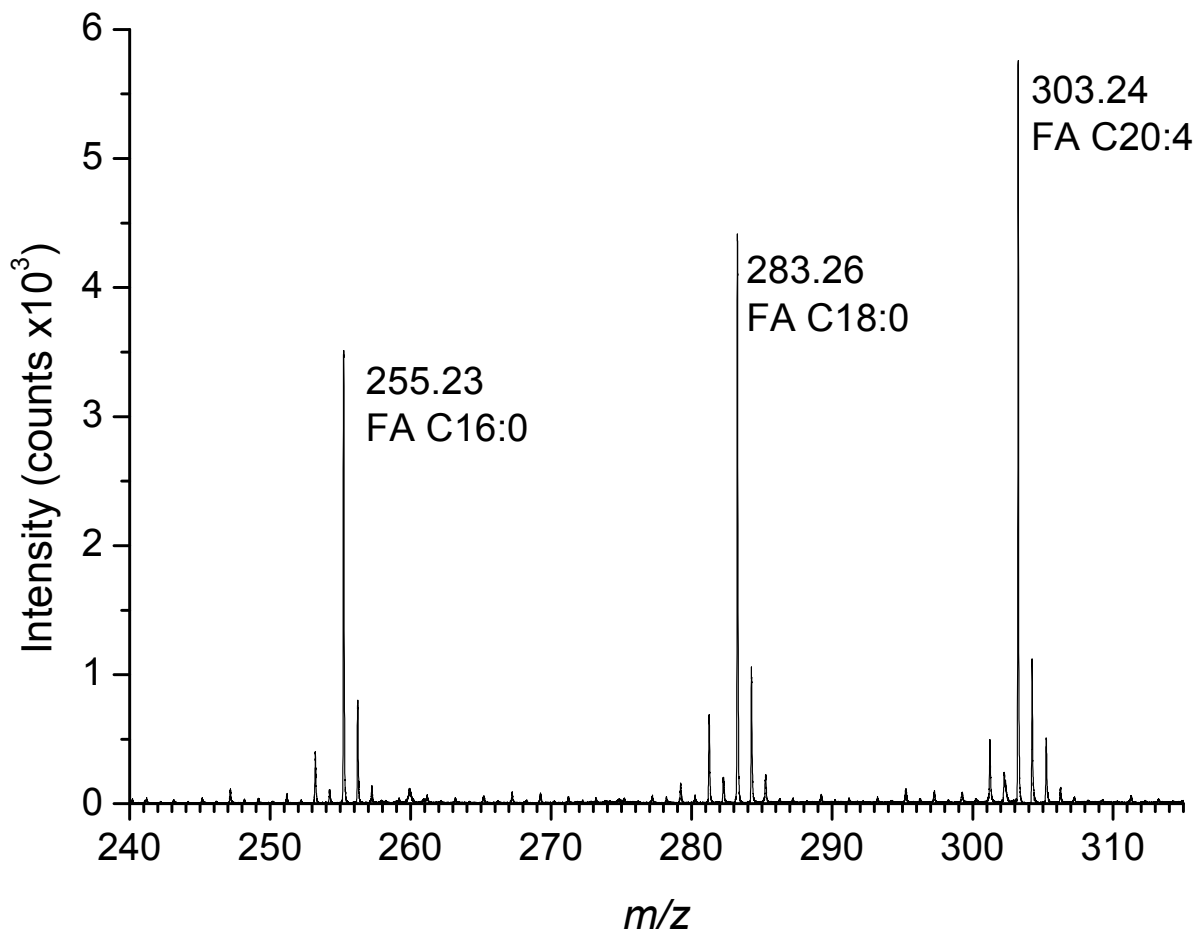


Figure S-1. ToF-SIMS negative ion mass spectrum of an equimolar mixture of palmitic (C16:0, MW 256.24 Da), stearic (C18:0, MW 284.24 Da) and arachidonic (C20:4, MW 304.24 Da) acids deposited on a silicon wafer.

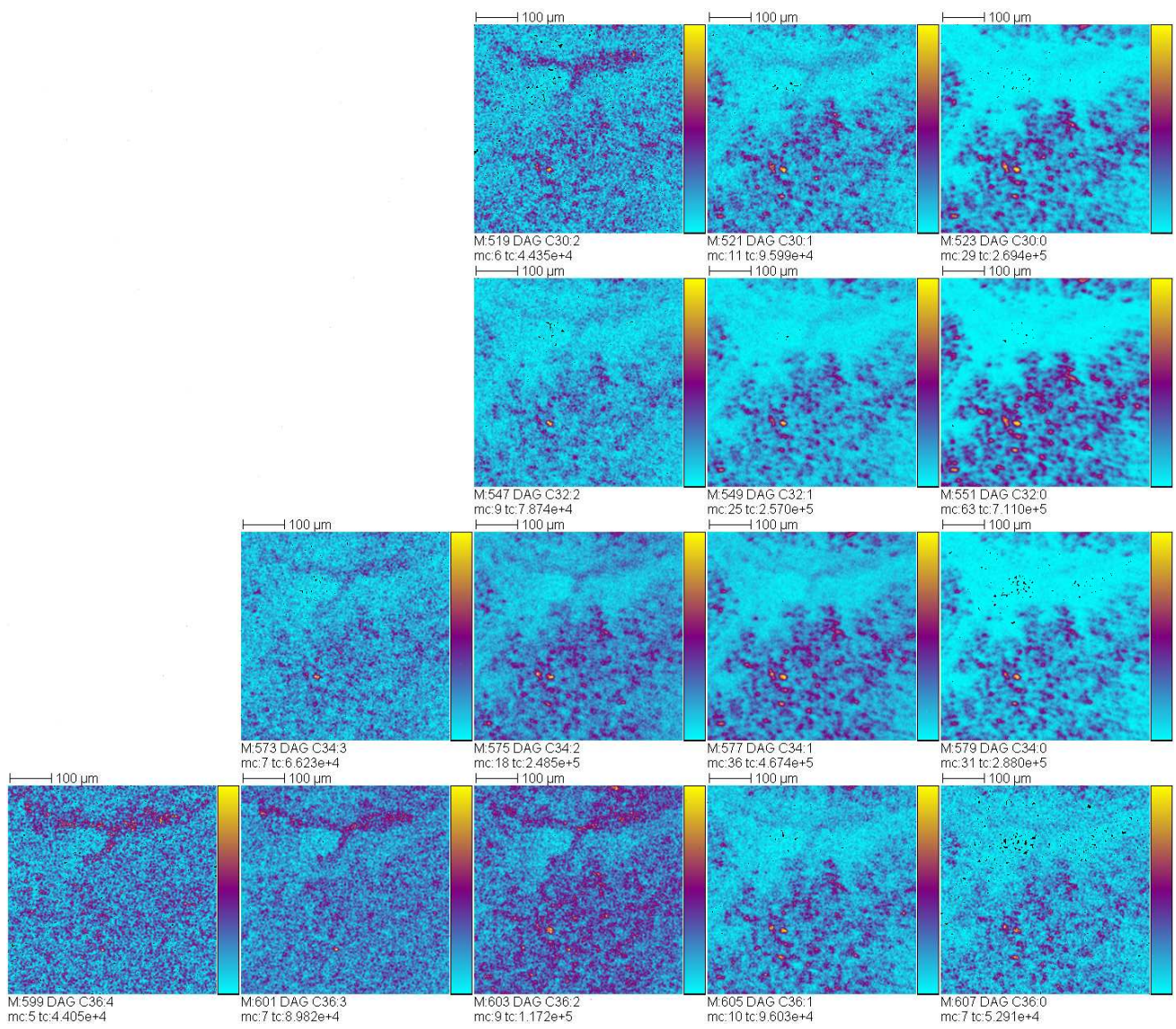


Figure S-2. Diacylglycerol positive ion images recorded from a non-steatosis area of a steatotic liver positive ion analysis. Color scale bars, with amplitude in number of counts, are indicated to the right of each ion image. The amplitude of the color scale corresponds to the maximum number of counts mc and could be read as [0, mc]. tc is the total number of counts recorded for the specified m/z (it is the sum of counts in all the pixels). Field of view: $500 \times 500 \mu\text{m}^2$.